

Fault Location with Load Profile Based Variation Compensation

Michael B. Orpilla¹, Russel John Gallano², Jordan Rel Orillaza²

¹ College of Engineering, Cagayan State University, Tuguegarao City Philippines

² Electrical and Electronics Engineering Institute, University of the Philippines-Diliman

Abstract — Accurate and fast location of the fault is essential in distribution system operation to ensure continuity and quality of power supply. Many impedance-based fault location (IBFL) techniques such as Equivalent Impedance Based (EIB) and Load Level Based (LLB) perform load variation compensation but assume a uniform percent load change across all connected loads; such assumptions are hardly applicable in distribution systems where various types of loads are connected. It was observed in this study that their accuracy reduces as the fault current becomes comparable to the load current. This research performs load variation compensation by considering the load profiles of the various types of loads connected in the distribution system. By doing this, loads are better represented in the simulation, which results in better prediction accuracy. The proposed method, Load Profile Based (LPB), is compared to EIB and LLB in simulations conducted in an actual distribution feeder from Cagayan II Electric Cooperative. The results show improved fault location having an average relative error based on line length (RELL) at a high-impedance-fault scenario ($Z_f=100$ ohms) not exceeding 3.22% compared to 48.74% (LLB) and 14.19% (EIB). In these techniques, a phasor measurement unit (PMU) is assumed to provide reference phasor voltage and currents at the root node. We further illustrate that additional PMU improves fault location by improving load variation compensation and faster fault location as PMU provides boundaries and effectively reduces the search space.

Keywords — Fault Location, Load Profile Based, Load Variation Compensation, PMU

I. INTRODUCTION

Shunt or series faults primarily caused by clustered trees, animal contacts, accidents, and or typhoons and earthquakes happen in distribution networks leading to power interruption. These result in revenue losses not only on the part of distribution utility, but also to its consumers. Fast and accurate fault location is thus necessary to address these issues. There are many improvements made in the impedance based fault location (IBFL) methods. Some of these address the effect of fault resistance [1], non-homogeneity of lines [2], unbalanced system [3], and fault on lateral sections [3, 4]. Multiple estimates or predictions are also problems considered in the development of IBFL techniques. Some researchers addressed this by utilizing remote fault indicators [5] and the status of the switches and breakers [6] installed along the distribution line. If no indicators are installed along the line, voltage sag mismatch [7] and error-index [8] are used to reduce multiple estimates.

With these developments, fault location may still be enhanced if we improve load compensation which has a significant effect especially with high fault impedance where fault currents may be comparable to load currents. In bolted fault, the fault current is much greater than load currents such that poor load representation hardly affects prediction accuracy.

However, at higher fault impedance, load currents have a significant contribution to the total fault current as measured from the source. This means that misrepresented loads by failure to consider load variation will increase the error of fault location. Some researchers compensate for load variation by using load-level based (LLB) compensation [9], equivalent impedance based (EIB) compensation [4], or current compensation [10]. LLB computes for the load level by comparing the measured pre-fault and the rated apparent power at the root node. This load level will be directly used to adjust the loads from their rated value. This, however, does not consider the effect of line loss in the computation and assume uniform load compensation across all connected loads. EIB performs power flow to accommodate line losses and performs load variation compensation by comparing equivalent impedance to the rated impedance; still assuming uniform load compensation across all connected loads. Such assumption is not applicable in an actual distribution system where different types of loads are connected. These loads operate at different patterns, so the assumption of uniform change should not be employed. Misrepresentation of these variations leads to less accurate fault location especially for high impedance faults. This research, Load Profile based (LPB) compensation improves IBFL techniques by accommodating various load profiles for various load types for a more accurate fault location even for higher impedance faults. The proposed method (LPB) is illustrated in two scenarios: using a single PMU at the root node and utilizing sparsely located PMU in the distribution line. Additional PMU will provide boundaries and subdivides the complex system into smaller sections. This facilitates faster fault location since it is no longer necessary to perform fault location for the entire feeder, but only on the identified faulted section. Also, additional measurement reduces load variation uncertainties, thus improving load variation compensation.

II. METHODOLOGY

Many improvements were made for the IBFL, but they still have limitations, particularly on variation compensation. Misrepresented load in the algorithm results in less accurate prediction particularly for higher fault impedance. In this section, the improved fault location algorithm is presented.

Distribution utilities have various feeders set up. Feeders in urban areas usually have multiple measurement points, while rural areas have a single measurement point located at the substation. The proposed improvement is discussed both for a single measurement and multiple measurement points.

2.1 Single Measurement with Load Profile Based (LPB) variation compensation

Figure 1 illustrates the major processes for a single-ended fault location. The data needed for this method are the following: pre-fault and fault current and voltage phasors at the substation, representative load profiles for each load type connected, and the feeder network data. The algorithm starts by performing load variation compensation for power mismatch from the pre-fault to the load defined in the load profile. A load flow is carried out next to solve for the voltages and currents for all the nodes and sections of the system. These voltages and currents are used to determine the equivalent circuit for all possible power flow paths (PPFP).

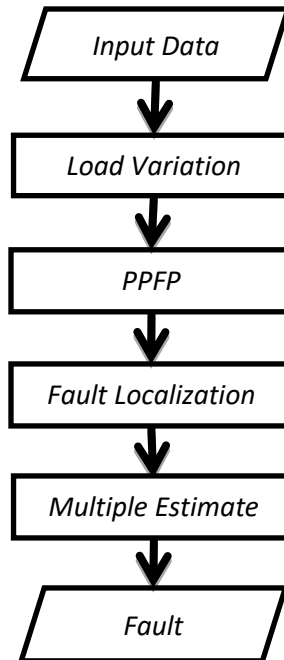


Figure 1. Single-ended Fault Location Process Flow

Lastly, per section fault location is performed for every PPFP. Multiple estimates are eliminated by using any of the techniques in subsections 2.1.5 depending on the available infrastructure in the given system. The algorithm is explained in more detail in the following subsections.

2.1.1 Load Variation Compensation

For this study, since the focus is on the primary side of the distribution system, all loads are lumped and referred to the primary side of the distribution transformer. The equivalent transformer load curves are derived from the load profiles of each load connected to it. The substation's load profile is determined through a time series (24-hr) load flow considering the 24-hour load profiles of all the loads connected. A higher resolution time-series load flow could be used for better load representation, however, the data available and provided by the DU (Figure A.1) is hourly, so this study is limited to hourly simulations.

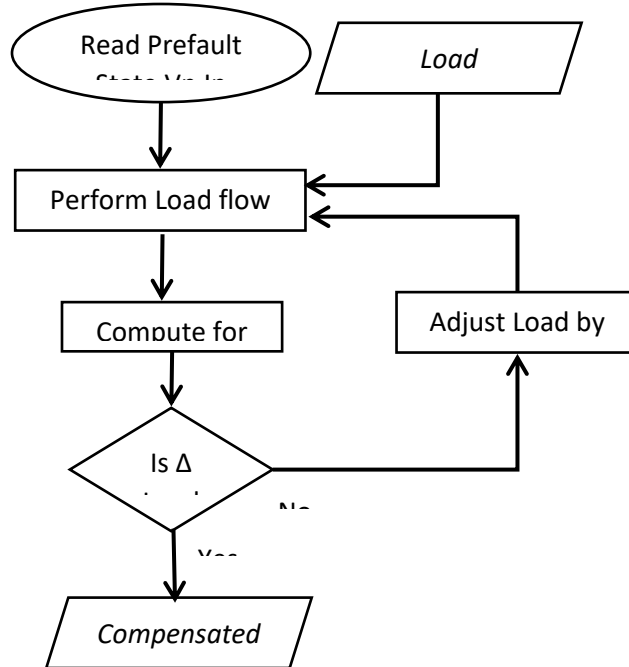


Figure 2: Load Variation Compensation Process Flow

Generally, the substation’s loading at a given time could be determined based on the substation’s load profile. Load variation compensation is carried out if the measured pre-fault apparent power is not equal to the apparent power based on the substation’s load profile. A Forward-Backward Sweep (FBS) load flow [16] initially considering the magnitude of loads connected based on its load profile at the time of fault occurrence is performed. At the substation, the apparent power computed S_{calc} (Eq.1) after the load flow and the measured pre-fault apparent power S_{meas} are used to solve the load variation (Δ_{load}) (Eq.2). If Δ_{load} is not within the error limit ($\epsilon \leq 1 \times 10^{-6}$), all the loads connected are modified (Eq.3) by multiplying the loads’ magnitude based on load profile by the change in loading ($1 - \Delta_{load}$) as illustrated in equation 3. Error limit of 1×10^{-6} , corresponding to only 10VA error, is justifiable for a 10MVA substation capacity. The iteration continues until Δ_{load} is within the defined error limit.

$$S_{calc} = V_{meas} I_{calc}^* \tag{1}$$

$$\Delta_{Load} = \frac{S_{calc} - S_{meas}}{S_{meas}} \tag{2}$$

$$Load_{Modified} = (Load_{Rated}) (Load_{PUT})(1 - \Delta_{Load}) \tag{3}$$

where:

- V_{meas} : measured pre-fault voltage
- S_{meas} : measured pre-fault apparent power
- S_{calc} : computed apparent power after pre-fault loadflow
- I_{scal} : computed source current after pre-fault loadflow
- $Load_{PUT}$: per unit load profile on the time of fault occurrence
- $Load_{Modified}$: Modified load after load variation compensation
- $Load_{Rated}$: Rated Load

The final compensated magnitudes of connected loads are used in the succeeding steps of the fault location algorithm. The existing methods, LLB and EIB, assume uniform percent change for all loads connected depending on the computed change at the substation side. This assumption is not applicable in distribution systems where different types of load are connected. The proposed method (LPB), however, compensates for load variation considering the load profiles of each type of load connected. This gives a better representation of the loads connected, resulting in better prediction accuracy. Appendix B shows the improvement in the load variation compensation of the proposed method against the existing methods for simulations conducted on a simple feeder containing three various types of load.

2.1.2 PFPF Equivalent Circuit Derivation

The technique of the Possible Power Flow Path (PFPF) equivalent circuit [4], [11] is adapted. The equivalent circuits for all the possible paths from the root node to a leaf node are determined. We illustrate PFPF in figure 3. Figure 3(a) shows a 13 bus sample feeder and figure 3(b) shows its equivalent PFPF for a path from the root node (bus1) to the leaf node (bus4). The laterals and sub-feeders outside the PFPF considered are converted into their equivalent load as describe in Eq.4.

$$Z_{eqk} = \frac{V_k}{I_{k-1,k} - I_{k,k+1}} \tag{4}$$

where:

- k : node considered
- Z_{eq} : thevenin equivalent impedance
- V_k : calculated pre-fault voltage from load flow
- $I_{k-1,k}$: upstream current of the node considered
- $I_{k,k+1}$: downstream current of the node considered

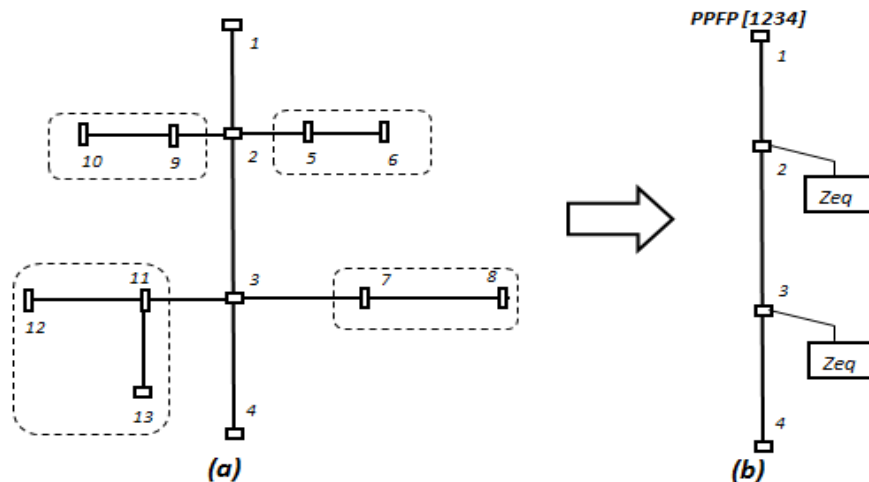


Figure 3: PFPF Determination

The total number of PPF from the sample feeder is six, equivalent to the total number of leaf nodes. Adopting this technique simplifies the fault location. In the succeeding steps, a loadflow downstream from the analyzed section is always carried out to determine the outgoing current from the assumed fault point. If the complex feeder is not converted into its equivalent PPF, it will take substantial amount of time performing this loadflow.

2.1.3 Per Section Fault location

Once load variation is compensated and the equivalent circuit for every PPF is derived, per section fault location [3] for every PPF is performed. This method is an iterative process performing a per section fault location from the root node towards the leaf node of every PPF. To better illustrate the process, consider a single line to ground fault on phase A that happened in a section between nodes m and n as presented in figure 4.

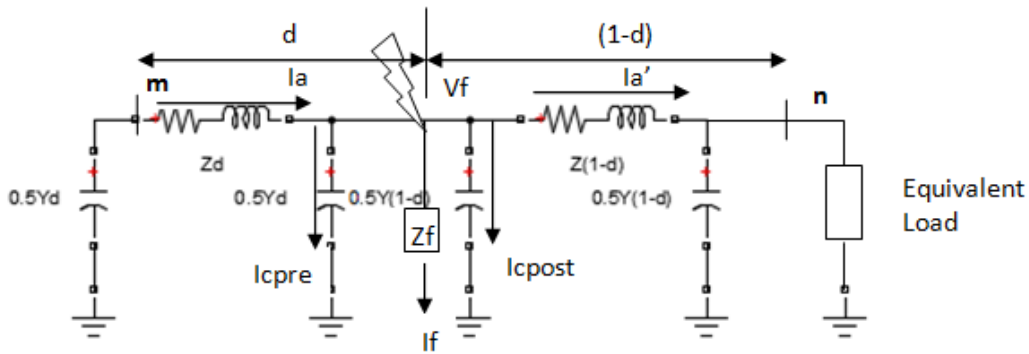


Figure 4: SLG fault illustration

The procedure is as follows:

1. With the given fault voltage and current, initially assume a value for the fault distance d (a good guess is 0.5) and solve for the voltage at the fault point, V_f .

$$V_f = V_m - d \cdot Z \cdot I \tag{5}$$

2. With the voltage at the fault point, compute for line capacitance currents I_{cpre} and I_{cpost} before and after fault point, respectively.

$$I_{cpre} = 0.5 \cdot Y \cdot d \cdot V_f \tag{6}$$

$$I_{cpost} = 0.5 \cdot Y \cdot (1 - d) \cdot V_f \tag{7}$$

3. With the voltage at the fault point, perform a downstream FBS power flow to solve for the outgoing 3-phase current I' then solve for fault current I_f (assume faulted phase is A).

$$I_{fa} = I_a - I_{cprea} - I_{cposta} - I'_a \tag{8}$$

4. With the solved value of fault current, a voltage equation on faulted phase is written as:

$$V_a = d * (I_a Z_{aa} + I_b Z_{ab} + I_c Z_{ac}) + I_{f_a} R_{f_a} \quad (9)$$

5. Split equation (9) into its real and imaginary components and solve for the fault distance (d) from node m

$$d = \frac{(V_{a_r} I_{f_{ai}} - V_{a_i} I_{f_{ar}})}{(M I_{f_{ai}} - N I_{f_{ar}})} \quad (10)$$

$$M = R_{aa} I_{a_r} - X_{aa} I_{a_i} + R_{ab} I_{b_r} - X_{ab} I_{b_i} + R_{ac} I_{c_r} - X_{ac} I_{c_i} \quad (11)$$

$$N = R_{aa} I_{a_i} + X_{aa} I_{a_r} + R_{ab} I_{b_i} + X_{ab} I_{b_r} + R_{ac} I_{c_i} + X_{ac} I_{c_r} \quad (12)$$

6. Check for convergence $\Delta d = d_l - d_{l-1}$; where lk = iteration
 7. Substitute the newly computed d in step 1 and keep on iterating until the value of d converges.
 8. If the final value of d after convergence is greater than one (1) per unit length, the fault is beyond the analyzed section. The voltage and current of the next section are updated as shown in equations 13 and 14, and follow the same process from Steps 1 to 8.
 9. However, if the final value of d is less than or equal to 1 per unit length, the fault is on the section analyzed. The total fault distance (Eq. 15) is the summation of the line length of the previous sections plus the actual distance from the analyzed section.

$$V_{k+1} = V_k - I_{l(k,k+1)} * Z_{k,k+1} \quad (13)$$

$$I_{l(k,k+1)} = I_{l(k-1,k)} - I_{load(k)} \quad (14)$$

$$D_{total} = d \cdot D_m + \sum_s^{m-1} D \quad (15)$$

where

Z : Line Impedance

Y : Line Admittance

V_f : Voltage at fault point

I_l : Line currents

I_{load} : Load currents

I_f : Fault Current

I : upstream current from fault point

I' : downstream current from fault point

I_{cpre} : Capacitance Current prior fault point

k : Node considered

V : Voltage

r : Real component;

i : Imaginary component

R_{jk} : Phase j & k mutual resistance

R_{kk} : Self Resistance at phase k

X_{jk} : Phase j & k mutual inductance

X_{kk} : Self Inductance at phase k

D : Distance

s : Substation bus

m : sending end node of faulted section

n : receiving end node of faulted section

2.1.4 Multiple Estimate Elimination

Since the method only uses a single measurement at the root node, multiple estimates or predictions are possible. These are locations that have the same electrical distance measured with the actual location of the fault. For instance, a fault happened at line sections 3-4 from the sample feeder in figure 3a it is also possible that the algorithm detects line sections 3-7 and 3-11 as faulted. The four methods below are proposed depending on the available infrastructure in the distribution system to single out multiple estimates.

- a) Voltage Sag mismatch [7]
- b) Use of Error Index [8]
- c) Detection of a section associated with fault thru the aid of Multi-Agent System (MAS) [6]
- d) Impedance based FL algorithm in conjunction with Software-based fault indicators [12]

Options (a) and (b) are used in case no other indicators are installed along the distribution line. Options (c) and (d) are adopted if there are already existing installed indicators and MAS. In this simulation, since the test feeder does not have any other indicators installed, Error Index [8] is used to break multiple estimates.

Single-ended FL needs a long time in finding the fault since it is required to perform fault location for all the possible paths. With the technological advancements, several distribution utilities today are deploying more meters like PMU along their distribution line. This meter is for monitoring the voltage and current phasors that are used in analyzing power quality, stability, and other network issues. This type of meter could also be used for fault location because of its high-resolution and GPS synchronized measurement.

2.2. Sparsely-Located PMU with Load Profile Based variation compensation

This paper also illustrates improvement of the single-ended LPB by utilizing sparsely located PMU in the distribution line. The number of PMU affects the accuracy and speed of fault location. More PMUs are needed to have a more accurate and faster fault location. However, installing more PMUs entail higher cost that most distribution utility could not afford. So to come up with a more accurate FL while minimizing cost, utilizing sparsely located PMUs is a good compromise.

Figure 5 shows the steps in fault location using sparsely located PMU. The method starts by determining the faulted section relative to the installed meter by comparing the pre-fault and the fault measurement of all installed PMUs. If a measured pre-fault current is greater than the fault current, the fault is upstream of that PMU; otherwise, it is downstream. With this information, it is easy to determine if the fault happened between two installed meters or downstream of the last meter. It is assumed that the node locations of PMUs and the loads connected downstream of them are known.

2.2.1 Faulted section is between two installed meters

If the faulted section is between two meters, load variation compensation is performed for loads between the two installed meters, then a two-ended fault location [13] is performed. Two-ended fault location determines only the faulted bus or line section along the

mainline where the two PMUs are connected. If the fault located is directly on the bus, then fault location validation is performed for any lateral directly connected to that bus. Single-ended fault location using the upstream PMU is performed for these lateral lines to verify whether the fault is on the main bus or along the lateral line.

2.2.2 *Faulted section is downstream of the last meter*

If the determined faulted section is downstream of a single PMU, load variation and single-ended fault location (same as in section 2.1) are performed on the line sections downstream of that PMU. This localized fault location facilitates the location of the fault.

Most of the steps in a single-ended FL location are adopted here. Only that the method could use either two-ended or localized single-ended fault location depending on the determined faulted section. With more meters, the uncertainty in load variation compensation is reduced, thus providing more accurate results. Together with the possibility of performing a localized fault location, a faster fault location is expected.

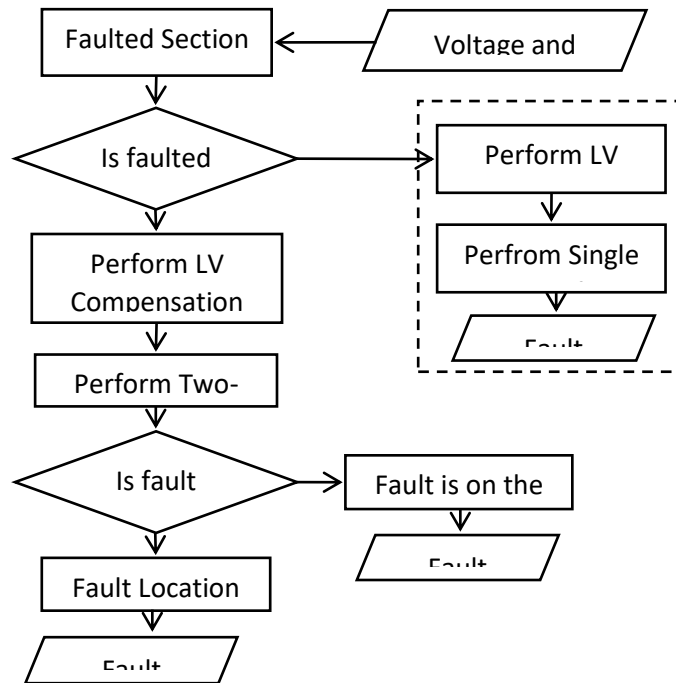


Figure 5: FL Flow chart considering sparsely located meters

III. RESULTS AND DISCUSSION

The proposed method Fault Location with Load Profile Based (LPB) variation compensation was tested and compared to existing methods: Load Level Based (LLB) and Equivalent Impedance Based (EIB). The comparison was made in the simulations conducted on an actual distribution feeder from Cagayan II Electric Cooperative. The actual test feeder in figure 6 was of radial type, has a primary line length of 38 km, and 11,448 consumers lumped across 133 distribution transformers. More details as to the load composition of the

test feeder and the hourly load profile were presented in Appendix A. We introduced +/- 20% uniformly-distributed variation about each value for the seven hourly load profiles used in this simulation.

Using Open DSS, distribution network analyses for the unbalanced three-phase feeder were performed. Load flow and fault simulation results were considered as known values and used as inputs to the fault location algorithm. The relative error based on line length (RELL) was the measure of accuracy used to compare the effectiveness of the proposed method with existing techniques. [17]

$$RELL = \frac{(Estimate - Actual)}{Feeder\ Line\ Length} \quad (16)$$

3.1. LLB, EIB and Single-Ended LPB Comparison

Two simulation cases were conducted in this study: fault at mainline (bus 74) and lateral line (bus 152) with the three different fault impedances: Low impedance ($Z_f = 0$), intermediate impedance ($Z_f = 25$), and High impedance ($Z_f = 100$). All the earlier discussions on LLB, EIB, and LPB under section 2.1 were single-ended techniques since a single PMU located at the S/S was used for reference. Faults conducted in this simulation were all located downstream from this reference. Using single measurement, the fault location was performed on all line sections for the entire feeder. The comparison of the hourly prediction accuracy of the existing against the proposed method were presented in figures 7 and 8 while the 24-Hr average REll were presented in tables 1 and 2 for cases 1 and 2, respectively.

Hourly prediction comparison and the average REll showed that the proposed method, Single-Ended LPB, outperformed both existing LLB and EIB methods. Existing methods could provide good results at bolted fault conditions, but error increases as the fault impedance increases as a result of less accurate load representation. At bolted fault, the measured current at the substation during fault was predominantly due to fault current. In this case, a misrepresented load has no significant effect on the fault location. However, the increased in the fault impedance resulted in a significant share of the load current in the total measured current at the substation. Say for a 100 ohms fault impedance for a single line to ground fault at a nominal line to neutral voltage of 7620V, fault current will be roughly about 80 Amperes, which is not very far from the usual size of loads in the feeder. In this case, misrepresented load will result to less accurate prediction. The proposed method showed significant improvement in the prediction accuracy. Its error also increased with fault impedance, but not as much as that for the LLB and EIB, because of better load representation.

Most of the time for higher fault impedance, LLB failed to converge due to large compensation error. It provided good results only at bolted fault and when the loads were operating near their rated values. EIB, on the other hand, had better prediction compared to LLB having an average REll at 100-ohm fault impedance of **14.19%** (*approximately 2200 meters*) for case 1 and **4.08%** (*approximately 650 meters*) for case 2. This prediction accuracy, however, is still behind that of the proposed method, single-ended LPB. LPB had

an average error for 100-ohm fault impedance of **3.22%** (approximately 500 meters) and **0.98%** (approximately 150 meters) for case 1 and case 2, respectively.

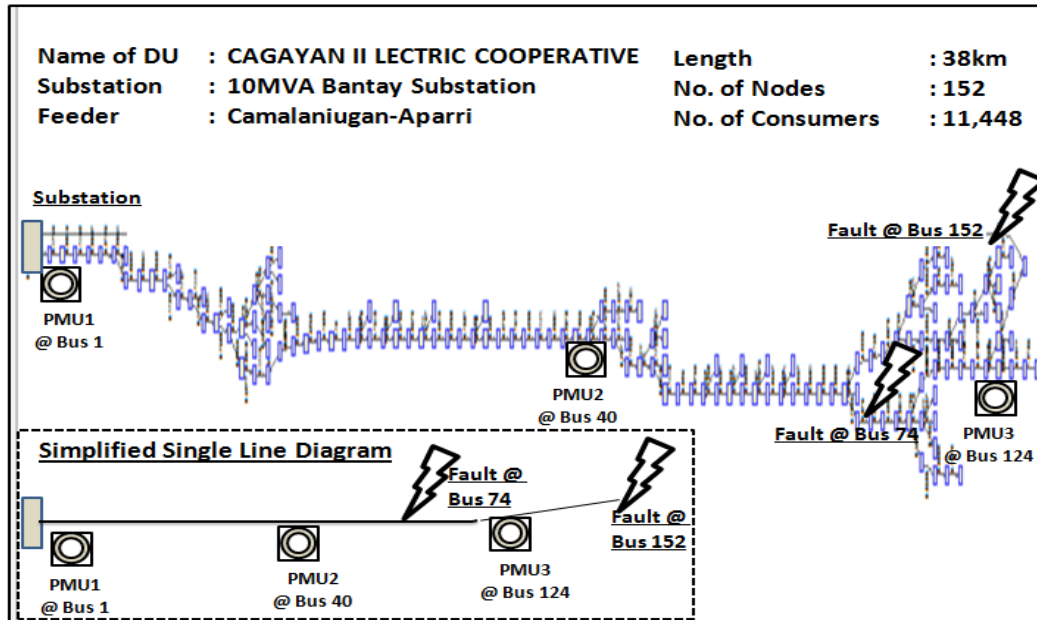


Figure 6: Single Line Diagram of Actual Test Feeder

Table 1: Average Relative Error based on Line Length (RELL) for fault at bus 74

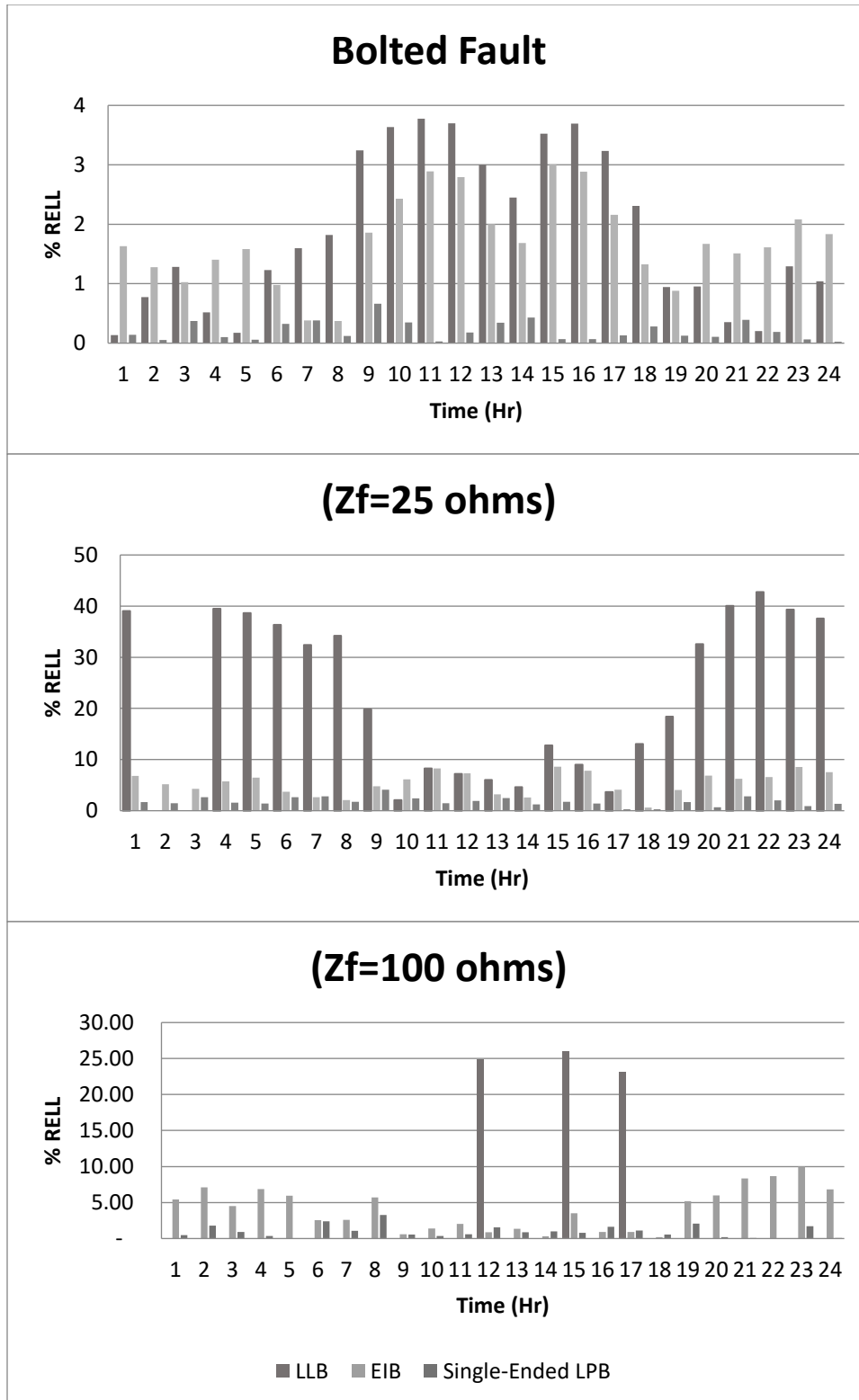
Fault Impedance (ohms)	LLB	EIB	Single-ended LPB
Z _f =0 (bolted)	1.87%	1.71%	0.21%
Z _f = 25	25.72%	5.42%	1.78%
Z _f = 100	Nan*	14.19%	3.22%

**Not a Number because there are periods where LLB failed to converge illustrating that this technique is ineffective when load current is comparable to fault current.*

Table 2: Average Relative Error based on Line Length (RELL) for fault at bus 152

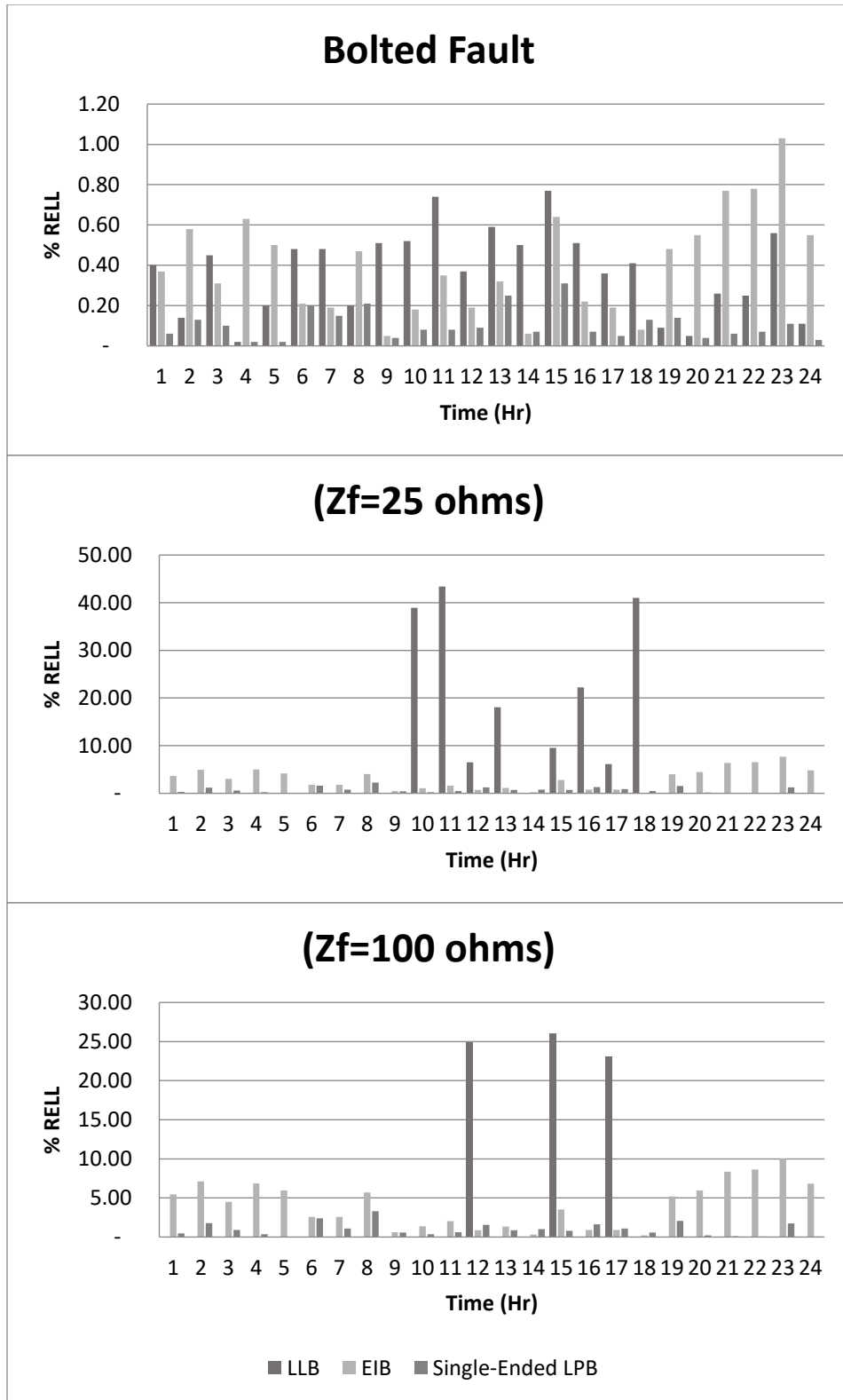
Fault Impedance (ohms)	LLB	EIB	Single-Ended LPB
Z _f =0 (bolted)	0.37%	0.40%	0.11%
Z _f =25	Nan*	3.00%	0.72%
Z _f =100	Nan*	4.08%	0.98%

**Not a Number because there are periods where LLB failed to converge illustrating that this technique is ineffective when load current is comparable to fault current.*



*Most of the time for a 100-ohm fault impedances, LLB failed to converged

Figure 7: Prediction accuracy comparison for fault at bus 74 (Mainline)



**Most of the time for 25-ohm & 100-ohm fault impedances, LLB failed to converged*

Figure 8: Prediction accuracy comparison for fault at bus 152 (Lateral)

3.2 Sparsely-Located PMU

Single-Ended LPB outperformed both the LLB and EIB, but this could be improved further by utilizing sparsely located PMUs installed in the distribution line. In this simulation, two more PMUs were added and installed at bus 40 (PMU 2) and bus 124 (PMU 3) as illustrated in figure 6. There were two possible scenarios of fault location using sparsely-located PMUs: fault in between two meters and fault downstream of the last meter. In these cases, two techniques could also be employed: two-ended fault location technique for faults that happened between two meters, while single-ended fault location for faults that happened downstream of the last meter. For the fault at bus 74, since it happened between PMU2 and PMU3, two-ended FL technique was used and only the lines and loads connected within this boundary were considered in the computation. For the case of fault at bus 152 on the lateral line, since it is located downstream of PMU3, only the lines and loads connected downstream of PMU 3 were considered in the fault location. Utilizing Sparsely-located PMUs in both cases resulted in faster fault location and better prediction accuracy since the loads to be compensated were minimized and the search areas were reduced.

Figures 9 and 10 compared the hourly prediction accuracy for the faults occurring at mainline and at lateral. The average %RELL were presented in table 3. Though the Single-ended LPB already provided improved results, faster and more accurate results could be achieved by utilizing sparsely located PMUs. The possibility of having a localized fault location, where loads and line sections considered in the fault location were minimized, will result in better load variation compensation and eventually better prediction.

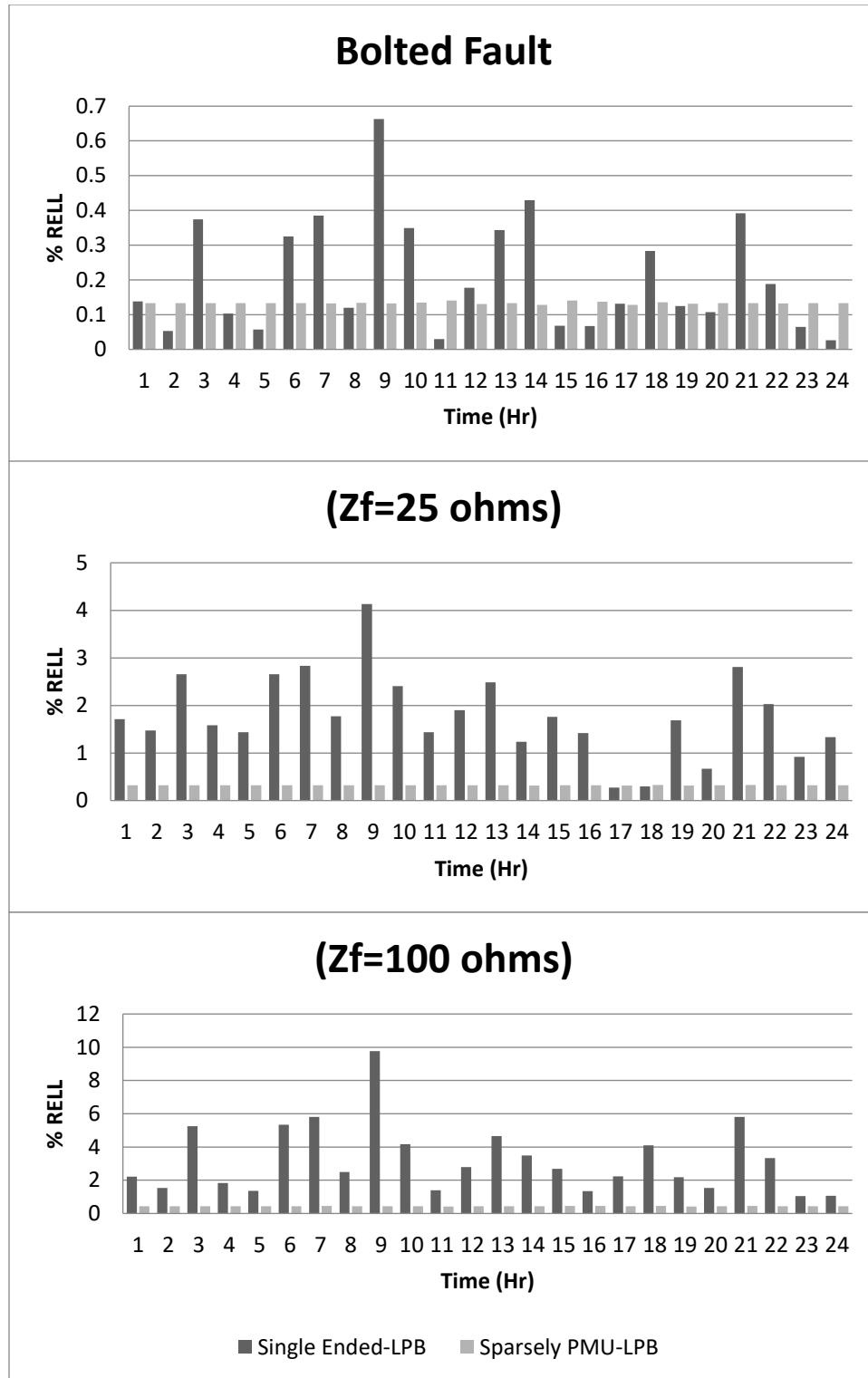


Figure 9: Prediction accuracy comparison for fault at bus 74 (Mainline)

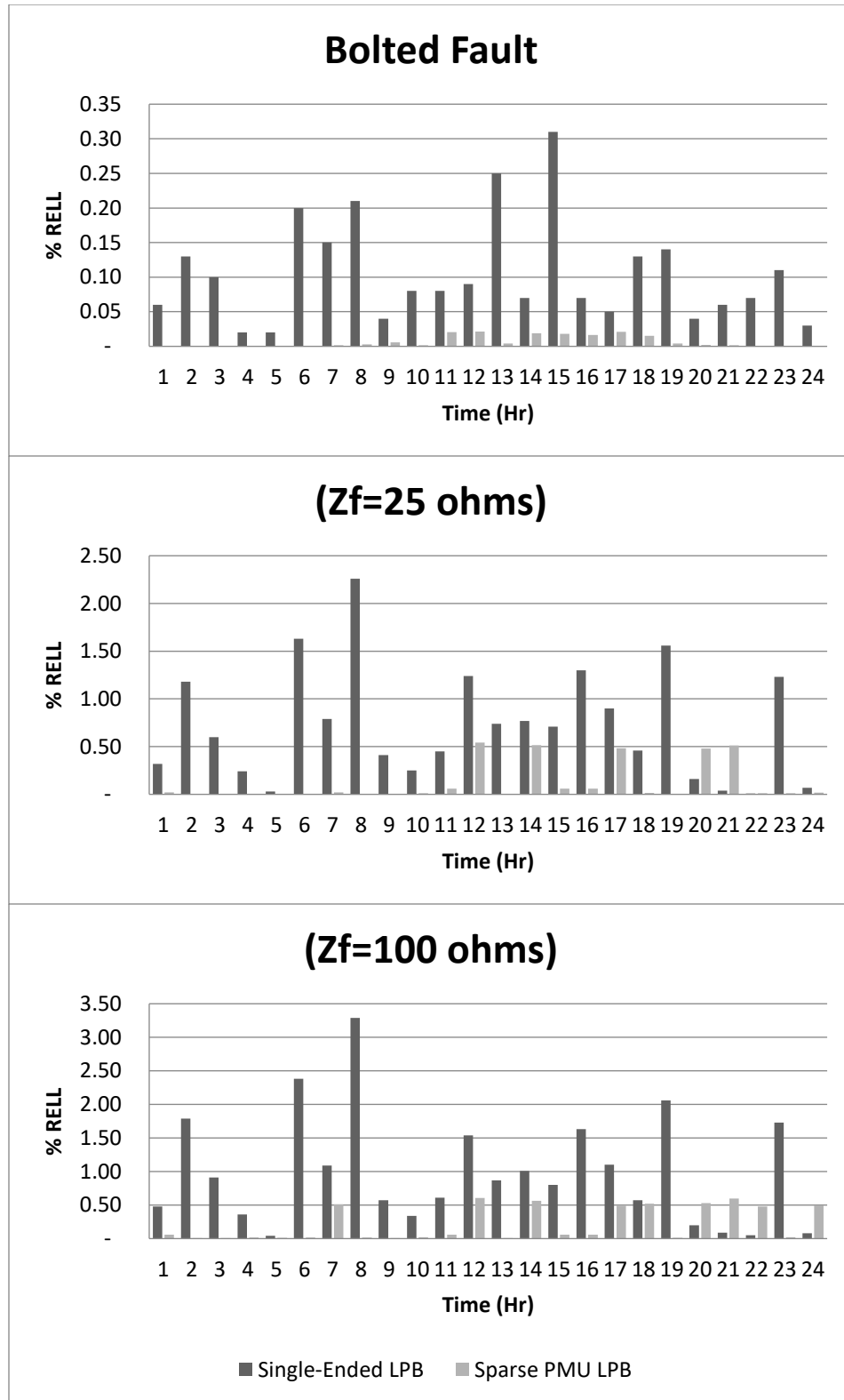


Figure 10: Prediction accuracy comparison for fault at bus 152 (Lateral)

Table 3: Average Relative Error based on Line Length (RELL)

Fault Impedance (ohms)	Fault at Bus 74 (Mainline)		Fault at Bus 152 (Lateral)	
	Single-ended LPB	Sparsely located PMU-LPB	Single-Ended LPB	Sparsely located PMU-LPB
$Z_f=0$ (bolted)	0.21%	0.13%	0.11%	0.01%
$Z_f= 25$	1.78%	0.32%	0.72%	0.12%
$Z_f= 100$	3.22%	0.43%	0.98%	0.22%

IV. CONCLUSIONS AND RECOMMENDATIONS

We have presented load variation compensation where load profiles for various types of loads were utilized to adjust loads for an impedance-based fault location algorithm. This method outperformed two existing methods: load level based (LLB) and equivalent impedance based (EIB) especially for cases of high impedance faults where fault current is comparable to the load current.

In these impedance-based methods, a PMU that provides reference voltage and current phasors at the root node is expected. We further showed in our analysis that utilizing additional PMU measurements, even at sparse locations throughout the feeder introduced a significant improvement to the fault location. The results showed that the proposed methods, Single-ended LPB and sparsely located PMULPB, have better prediction accuracy than the existing methods, they have an average RELL not exceeding 3.22% and 0.43% respectively, even for fault impedance as high as 100 ohms. These errors correspond to only 500 and 75 meters, respectively.

For faster and better prediction accuracy, it is recommended to consider more and higher resolution load profiles and installation of more PMUs. This paper is successfully tested in a single source radial system, its application to multi-source systems together with the inclusion of seasonal effect of loads is recommended.

VI. ACKNOWLEDGEMENTS

The authors wish to acknowledge the assistance of Cagayan II Electric Cooperative for providing the Test feeder needed in this study.

References

- [1] Zimmerman K, Costello D. 2006. Impedance-based fault location experience. Proceedings of the IEEE Rural Electric Power Conference; Albuquerque, NM, USA. IEEE. doi: 10.1109/REPCON.2006.1649060.
- [2] Saha MM, Provoost F, Rosolowski E. 2001. Fault location method for MV cable network. 2001 Seventh International Conference on Developments in Power System Protection (IEE);Amsterdam, Netherlands. IET. p. 323-326. doi: 10.1049/cp:20010165
- [3] Zhu J, Lubkeman DL, Girgis AA. 1997. Automated fault location and diagnosis on electric power distribution feeders. IEEE Transactions on Power Delivery; 12(2) 801-809. Available from: <https://ieeexplore.ieee.org/document/584379>.
- [4] Salim RH, Resener M, Filomena AD, Caino de Oliveira KR, Bretas AS. 2009. Extended fault-location formulation for power distribution systems. IEEE Transactions on Power Delivery. 24(2): 508-516. Available from: <https://ieeexplore.ieee.org/document/4797797>.
- [5] Das R, Sachdev MS, Sidhu TS. 2000. A fault locator for radial subtransmission and distribution lines. 2000 Power Engineering Society Summer Meeting (Cat. No.00CH37134); Seattle, WA, USA. IEEE. 1: 443-448. doi: 10.1109/PSS.2000.867627.
- [6] Zheng T, Jia H. 2011. Application of multi-agent and impedance-based algorithm for fault location in power distribution systems with DG. 2011 International Conference on Advanced Power System Automation and Protection; Beijing, China. IEEE. p. 1044-1049. doi: 10.1109/APAP.2011.6180703.
- [7] Estebansari A, Pons E, Bompard E, Bahmanyar A, Jamali S. 2016. An improved fault location method for distribution networks exploiting emerging LV smart meters. 2016 IEEE Workshop on Environmental, Energy, and Structural Monitoring Systems (EESMS); Bari, Italy. IEEE. p. 1-6. doi: 10.1109/EESMS.2016.7504815.
- [8] Ramar K, Ngu EE. 2010. A new impedance-based fault location method for radial distribution systems. IEEE PES General Meeting; Minneapolis, MN, USA. IEEE. p. 1-9. doi: 10.1109/PES.2010.5588189.
- [9] Gabr MA, Ibrahim DK, Ahmed ES, Gilany MI. 2016. A new impedance-based fault location scheme for overhead unbalanced radial distribution networks. Electric Power System Research. 1st ed. 142: 153-162. <https://doi.org/10.1016/j.epsr.2016.09.015>
- [10] Mora-Florez JJ, Herrera-Orozco RA, Bedoya-Cadena AF. 2014. Fault location considering load uncertainty and distributed generation in power distribution systems. IET Generation, Transmission and Distribution. 9(3): 287-295. <https://doi.org/10.1049/iet-gtd.2014.0325>.
- [11] Resener M, Salim RH, Filomena AD, Bretas AS. 2008. Optimized fault location formulation for unbalanced distribution feeders considering load variation. 16th Power Systems Computation Conference, Glasgow, Scotland. p. 500-506
- [12] Das R. 1998. Determining the location of faults in distribution systems [doctoral]. Saskatchewan, Saskatoon: University of Saskatchewan.
- [13] Ramírez-Ramírez J, Mora-Florez J, Grajales-Espinal C. 2015. Fault location method based on two end measurements at the power distribution system. 2015 IEEE 6th Latin American Symposium on Circuits & Systems (LASCAS); Montevideo, Uruguay. IEEE. p. 1-4. doi: 10.1109/LASCAS.2015.7250475.
- [14] Ghaderi A, Mohammadpour HA, Ginn HL and Shin Y. 2014. High-impedance fault detection in the distribution network using the time-frequency-based algorithm. IEEE Transactions on Power Delivery. 30(3): 1260-1268. Available from: <https://ieeexplore.ieee.org/document/6915897>.
- [15] Kersting WH, PhillipsWH. 1994. Distribution feeder line models. Proceedings of 1994 IEEE Rural Electric Power Conference; Colorado Springs, CO, USA. IEEE. p. A4/1-A4/8. doi: 10.1109/REPCON.1994.326257.
- [16] Kersting WH. 2017. Distribution system modeling and analysis. 4th ed. CRC Press.
- [17] IEEE Guide for Determining fault location on AC transmission and distribution lines. IEEE Std C37.114-2014 (Revision of IEEE Std C37.114-2004). p.1-76. doi: 10.1109/IEEESTD.2015.7024095.